Supplementary Figure 1

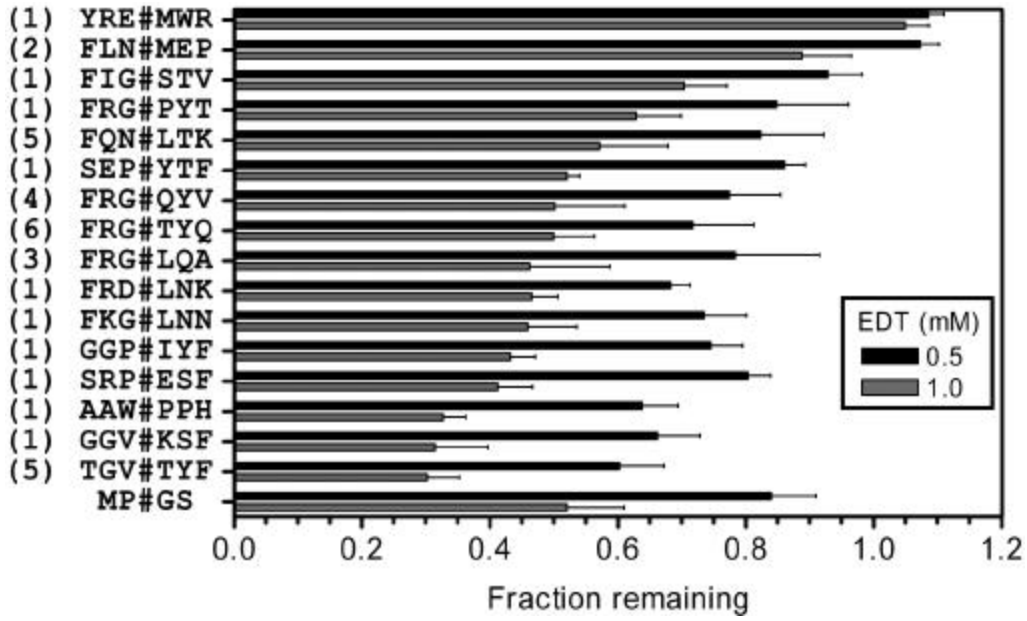

Supplementary Figure 1. Analysis of unique sequences isolated in Sort 14. Unique sequences are listed next to their frequency of occurrence, in parenthesis. Dithiol resistance is shown as the fraction of the FRET ratio remaining following washes with high concentrations of EDT, and corresponding standard deviations calculated from three or more duplicate wells on a 96-well plate.

Supplementary Figure 2

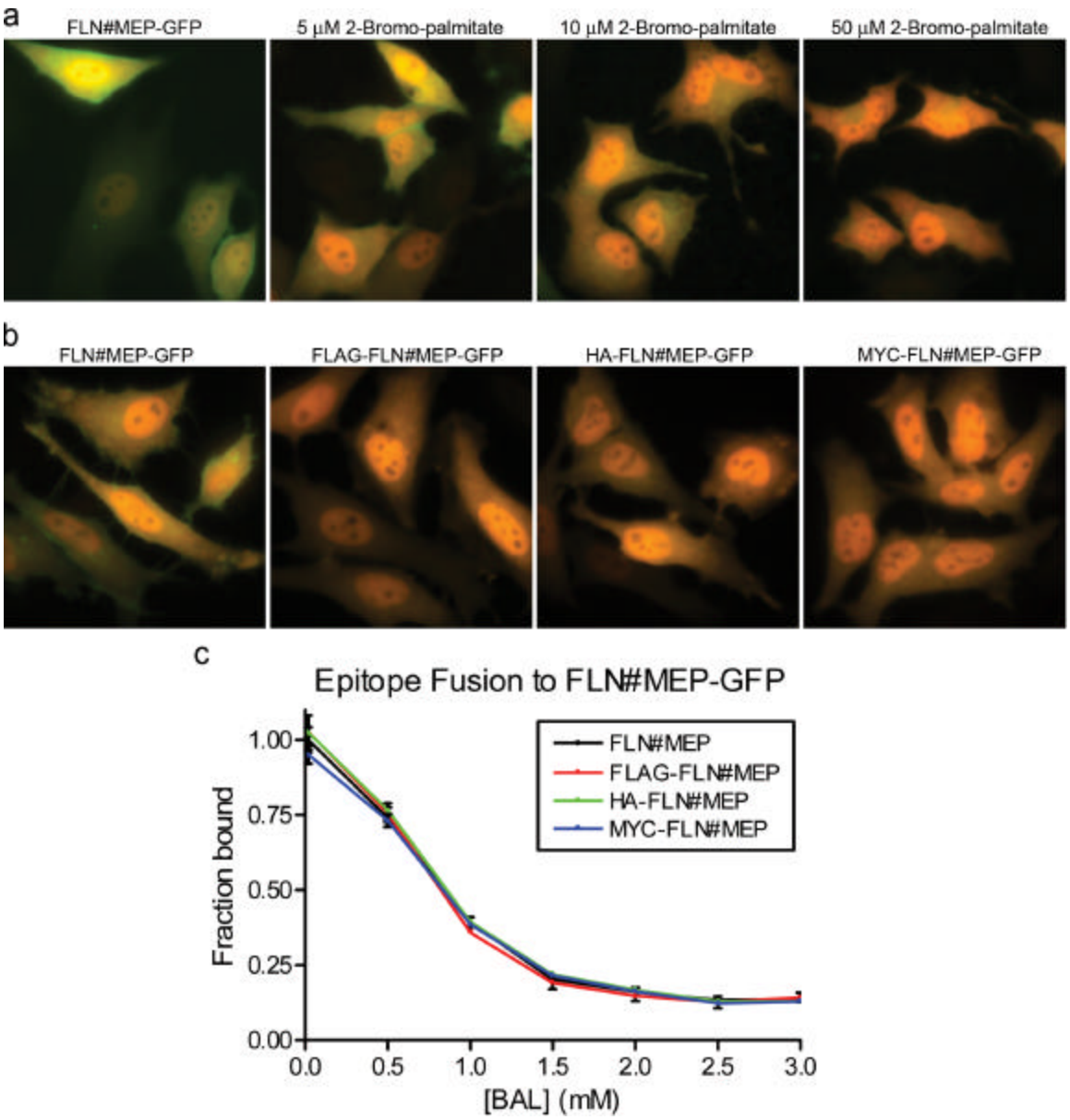

Supplementary Figure 2. Inhibition of tetracysteine-specific membrane localization. (a) Inhibition of membrane localization by addition of 2-bromopalmitate. HeLa cells were transduced with FLN#MEP-GFP virus in media containing increasing concentrations of 2-bromopalmitate (Fluka). Two days later, cells were ReAsH stained and imaged on a Zeiss Axiovert 200M microscope with a cooled charge-coupled device camera (Roper Scientific), controlled by METAFLUOR 6.1 software (Universal Imaging). Imaging of the tetracysteine-GFP fusion was achieved by using a 480/30 nm excitation filter, 505 nm dichroic mirror, and two emission filters (535/45 nm for GFP and 653/95 for ReAsH). The two emission images were scaled and combined as individual channels for GFP (green) and GFP-mediated FRET to ReAsH (red). (b) Addition of various

epitope tags N-terminal to the tetracysteine block palmitoylation and membrane localization in HeLa cells. Epitope fusions were generated by PCR and cloned into pCLNCX-WPRE to generate the following fusion proteins: (FLAG) MDYKDDDDKGS-FLN#MEP-GFP (Primer20, Primer10), (HA) MVYPYDVPDYAGS-FLN#MEP-GFP (Primer21, Primer10), (MYC) MVQKLISEEDLGS-FLN#MEP-GFP (Primer22, Primer10). HeLa cells were transduced with recombinant virus then two days later ReAsH stained and imaged. (c) Palmitoylation inhibition by epitope tag fusion does not affect the dithiol resistance of FLN#MEP performed as previously described. Similar results were observed for HRW#KTF.

Supplementary Figure 3

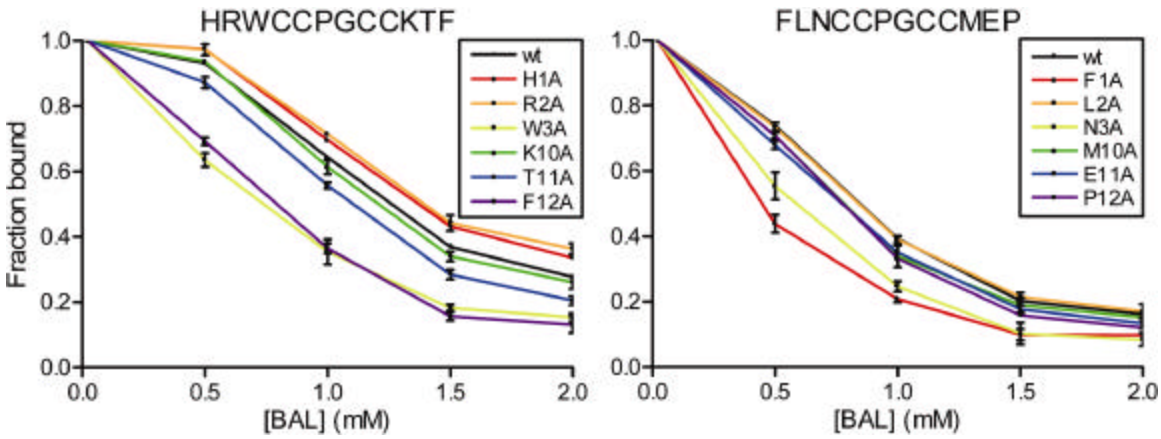

Supplementary Figure 3. Dithiol resistance of alanine mutants point to key residues. Alanine mutants of HRW#KTF-GFP (left) and FLN#MEP-GFP (right) were transduced into HEK293T cells and analyzed for dithiol resistance on a plate reader. All data points differ from wild-type to statistical significance ($P < 0.05$ by a two-tailed t-test) except FLN#MEP L2A at all concentrations of BAL tested, FLN#MEP M4A at 1.5 mM and 2.0 mM BAL, and HRW#KTF K4A at 1.0 mM and 1.5mM BAL. Data shown normalized to **Figure 2** titrations. In both sequences, hydrophobic aromatic residues such as Trp and Phe were found to be essential. These residues alone are insufficient to explain the high dithiol resistance phenotype, since each of the sequences isolated in the high FRET ratio population show a similar Phe at the first or last variable position or a Trp at the third variable position (see **Supplementary Figure 1** online), yet all are still less than optimal. HRW#KTF contains both a Trp and Phe, which in combination may lead to the observed superior dithiol resistance. Equally important in FLN#MEP is the Asn. Overall, the Ala scan demonstrates that each residue except the Leu contributes at least partially to the enhanced dithiol resistance of FLN#MEP. As for HRW#KTF, all residues contribute except the His and Arg, whose replacement by Ala slightly increases the dithiol resistance. Stacking of a tryptophan indole ring is known to quench fluorescein bound to anti-fluorescein antibodies[S1], so it is surprising that tryptophan immediately adjacent to a cysteine pair in HRW#KTF is compatible with, let alone contributory towards high quantum yield for ReAsH. These residues may have further roles in modulating the expression or fluorescent properties of the biarsenical-tetracysteine complex.

Supplemental References

S1. Watt,R.M. & Voss,E.W. Mechanism of Quenching of Fluorescein by Anti-Fluorescein IgG Antibodies. *Immunochemistry* **14**, 533-541 (1977).

Supplementary Table 1

Tetracysteine	FlAsH Quantum Yield on CFP		ReAsH Quantum Yield on GFP	
	N-terminus	C-terminus	N-terminus	C-terminus
αPG	nd	0.59	nd	0.28
MP#GS	0.72	0.50	0.30	0.18
HRW#KTF	0.65	0.61	0.40	0.34
FLN#MEP	0.78	0.70	0.47	0.42

Supplementary Table 1. Quantum yields of FlAsH and ReAsH bound to optimized tetracysteine sequences fused to fluorescent proteins. Fluorescent protein quantum yields were unaltered by fusion to the tetracysteine. Furthermore, synthetic FLN#MEP-amide gave extinction coefficients and quantum yields for both bound FlAsH (70,000 $M^{-1}cm^{-1}$ and 0.85) and ReAsH (69,000 $M^{-1}cm^{-1}$ and 0.48) equivalent to or slightly higher than the genetically encoded fusions to GFP. The pK_a's of FlAsH (5.5) and ReAsH (4.7) bound to were little changed from earlier peptides[6]. Oxidation of the Met to the sulfoxide barely changed the extinction coefficients or quantum yields.

Supplementary Table 2 Oligonucleotide primer sequences

Primer	Sequence
1	GATCCNNKNNKTGCTGCNNKNNKTGCTGCNNKNNKTAAGC (5'Phosph)
2	GGCCGCTTAMNNMNNGCAGCAMNNMNNGCAGCAMNNMNNG (5'Phosph)
3	ATTTTATAGCGGCCGCTTAGGATCCACTGCTTTCCTTGGTACAGCTCGTCCATGCCGAGAG
4	CCCAAGCTTGCCACCATGGTGAGCAAGGGCGAGGAG
5	TTTGGATCCNNKNNKNNKTGCTGCCCCGGCTGCTGC
6	TTTTGCGGCCGCCMNNMNNMNNGCAGCAGCCGGGGCAGCA
7	AATACGACTCACTATAGGGA
8	GTAATCCAGAGGTTGATTCTCGAGAAAA
9	TTTTAAGCTTGCCACCATGGCCGGATCCTAAGCGGCCGCAGCAAGGGCGAGGAGCTG
10	CCCCATCGATCTCGAGTTACTTGTACAGCTCGTCCAT
11	ACCTACAGGTGGGGTCTTTCATTCCC
12	AGCTCGTTTAGTGAACCGTCAGATC
13	GACAAGCGGCCGCTTAAGAACCGC
14	AAACTCGAGTTAGCGGCCGCCCCTCCACATGCAG
15	AAAGCGGCCGCCAGAACCGCAGCACCCGGGGCA
16	TTTGCGGCCGCATGGATGATGATATCGCCGCG
17	TTTCTCGAGCTAGAAGCATTTGCGGTGGAC
18	CTCAGATCTCGGGCTATGGATGATGATATCGCCGC
19	TCGAGATCTGAGTCCGGACTTGTACAGCTCGTCCATG
20	TTTAAGCTTGCCACCATGGATTACAAGGATGACGACGATAAGGGATCCGCCGGATCCTTTTTGAATTG
21	TTTAAGCTTGCCACCATGGTGTACCCCTACGACGTGCCCGACTACGCCGGATCCGCCGGATCCTTTTTGAATTG
22	TTTAAGCTTGCCACCATGGTGCAGAAGCTGATCTCAGAGGAGGACCTGGGATCCGCCGGATCCTTTTTGAATTG